Amyloid Fibril Formation Can Proceed from Different Conformations of a Partially Unfolded Protein

Martino Calamai,* Fabrizio Chiti,† and Christopher M. Dobson*
*Department of Chemistry, University of Cambridge, Cambridge CB2 1EW, United Kingdom; and †Dipartimento di Scienze Biochimiche, Università degli Studi di Firenze, 50134 Firenze, Italy

ABSTRACT Protein misfolding and aggregation are interconnected processes involved in a wide variety of nonneuropathic, systemic, and neurodegenerative diseases. More generally, if mutations in sequence or changes in environmental conditions lead to partial unfolding of the native state of a protein, it will often aggregate, sometimes into well-defined fibrillar structures. A great deal of interest has been directed at discovering the characteristic features of metastable partially unfolded states that precede the aggregated states of proteins. In this work, human muscle acylphosphatase (AcP) has been first destabilized, by addition of urea or by means of elevated temperatures, and then incubated in the presence of different concentrations of 2,2,2, trifluoroethanol ranging from 5% to 25% (v/v). The results show that AcP is able to form both fibrillar and nonfibrillar aggregates with a high β-sheet content from partially unfolded states with very different structural features. Moreover, the presence of α-helical structure in such a state does not appear to be a fundamental determinant of the ability to aggregate. The lack of ready aggregation under some of the conditions examined here is attributable primarily to the intrinsic properties of the solutions rather than to specific structural features of the partially unfolded states that precede aggregation. Aggregation appears to be favored when the solution conditions promote stable intermolecular interactions, particularly hydrogen bonds. In addition, the structures of the resulting aggregates are largely independent of the conformational properties of their soluble precursors.

INTRODUCTION

Many systemic and neurodegenerative disorders, from light chain amyloidosis to Alzheimer's disease, have been found to be associated with the misfolding and aggregation of specific proteins (1–3). There are thought to be two primary origins of the pathogenic behavior associated with these disorders: organ damage resulting from deposition of large amounts of fibrillar aggregates (4), generally called amyloid fibrils or plaques, and cellular dysfunction resulting from the interactions of small, perhaps nonfibrillar aggregates with plasma membranes and other cellular and extracellular components (2,5,6). Importantly, the latter species appear, at least in many cases, to represent the precursors of amyloid fibril formation (1,7,8).

Despite a lack of identifiable common features in the sequences and structures of the proteins implicated in the different amyloid diseases, the fibrillar aggregates associated with them are all characterized by a high degree of structural order and a high intermolecular β-sheet content (9–11). It has therefore been postulated that there is a common underlying mechanism of formation of the various fibrillar aggregates (1). Moreover, an increasing body of evidence supports the ''generic hypothesis'' that the ability to form amyloid structures with ordered intermolecular β-sheets is an inherent property of polypeptide chains and therefore that all proteins, at least in principle, have the potential to form such structures under appropriate conditions (1,10,12–14). The soluble precursors of amyloid aggregates can be either globular proteins, or their fragments, or natively unfolded polypeptides (15). Globular proteins generally need to be destabilized (e.g., by mutation (16–20), heat (21,22), high pressure (23,24), low pH (25,26), or organic denaturant (13,21)) to aggregate rapidly, with fibril formation proceeding either from extensively or partially unfolded states (1,15) or, in some cases, from native-like states in which unfolding may initially be limited and confined to local regions of the protein (27–30). By contrast, natively unfolded proteins expose large portions of their polypeptide chains to solvent so that aggregation, under conditions favoring intermolecular interactions, can occur without the prerequisite of a major conformational change (15).

A great deal of attention has recently been focused on the structural characteristics of the conformational states populated under conditions where aggregation occurs and on the factors that promote the conversion of these precursor states into aggregates (15,31–39). Electrostatic repulsion, hydrophobicity, and secondary structure propensity have all been shown to have a major influence on the tendency of fully or partially unfolded proteins to aggregate (35). Interesting issues in such studies are whether a high population of a specific conformation in denatured states is required for the efficient generation of amyloid fibrils and whether or not differences in the morphologies of the resulting fibrils are associated with differences in the structures and properties of the precursor states (34). Several studies have highlighted the fact that partially folded states containing α-helical structure are highly populated under conditions in which amyloid formation occurs, and indeed in some cases it is only at later

Submitted June 14, 2005, and accepted for publication September 6, 2005.

Address reprint requests to Christopher M. Dobson, E-mail: cmd44@cam.ac.uk.

0006-3495/05/12/4201/10 $2.00

doi: 10.1529/biophysj.105.068726

stages of the aggregation process that large-scale conversion to β-sheet structure takes place (40–45). In addition, it has been found that, depending on solution conditions, the presence of α-helical structure in partially folded states can promote the formation of fibrils as well as inhibit it (43). In other cases, however, it appears that aggregation involves the interaction between solvent-exposed and flexible regions that lack stable hydrogen-bonded elements of secondary structure, i.e., from highly unfolded polypeptide segments that can readily form β-sheet structure (18,22,39). Finally, as mentioned above, several recent studies show that in some cases aggregation can be initiated from highly native-like states before major conformational rearrangements (27–30,41).

To investigate further the relevance of the quantity and type of residual structure in the unfolded or partially unfolded states from which the aggregation process takes place, we have studied the effects of the nature of partially unfolded conformations, obtained under a range of conditions, on the aggregation behavior of human muscle acylphosphatase (AcP). AcP is a small globular protein shown to form fibrillar aggregates after partial unfolding in 25% (v/v) 2,2,2 trifluoroethanol (TFE) (13), a solvent that has been found also to promote aggregation of other polypeptides (46–50), including the natively unfolded Aβ-peptide (43). The resulting fibrils have a high content of β-sheet structure, bind to thioflavin T (ThT), and display apple-green birefringence in the presence of Congo red under cross-polarized light (13); this set of properties is highly characteristic of amyloid structures. In a variety of studies, TFE has been shown to stabilize hydrogen bonds but at the same time to weaken hydrophobic interactions (51–54). Different concentrations of TFE are therefore expected to give rise to different conformational distributions within partially unfolded states with a different ratio of α-helical/disordered structure and a variable degree of hydrophobic interactions.

The aggregation of denatured AcP has been found to be slow at concentrations of TFE higher than ~35% (v/v), and AcP is predominantly in its native state at concentrations below 18% (v/v) TFE at 25°C (19). We therefore carried out experiments in solutions having a range of TFE concentrations between 0% and 25% (v/v), after previously destabilizing the protein by an increase in temperature or by addition of urea. In this way, a range of different conditions was generated in which the protein is denatured but where noncovalent intermolecular interactions are still sufficiently favorable for the formation of aggregates. The results show that the aggregates formed from the differently structured denatured states of AcP share similar characteristics and that, at least in the case of AcP, the extent of α-helical structure in the denatured state is not a critical determinant of the ability to form amyloid fibrils under specific conditions. Taken together, these data indicate that a specific conformational state is not required to form ordered aggregates, provided that the solution conditions permit relatively stable intermolecular interactions.

MATERIALS AND METHODS

Protein production and purification

Expression and purification of wild-type AcP and the F94L variant were carried out according to the procedures described previously (55). A QuikChange Stratagene (La Jolla, CA) kit was used for site-specific mutagenesis, and DNA sequencing was used to ensure the presence of the desired mutations. The cysteine residue at position 21 was replaced by serine to avoid complexities arising from the presence of a free cysteine residue; the resulting mutant is described here as the wild-type protein as in previous studies (56). Protein concentrations were measured by ultraviolet (UV) absorption using ε_{280} values of 1.49 ml mg^{-1} cm^{-1}.

Aggregation kinetics

The rates of aggregation of the AcP variants were measured as previously described (57). In brief, for each experiment 60 μl aliquots of the sample were mixed at regular time intervals with 440 μl of 50 mM acetate buffer, pH 5.5, 25°C, containing 25 μM ThT. A Varian Cary Eclipse spectrofluorimeter (Palo Alto, CA) with excitation and emission wavelengths of 440 and 485 nm, respectively, was used to determine ThT fluorescence values. Single exponential functions were fitted to the kinetic plots reporting the measured ThT fluorescence versus time to determine the aggregation rate constants.

Circular dichroism

Circular dichroism (CD) spectra were recorded on a Jasco J-710 spectropolarimeter (Great Dunmow, Essex, UK) equipped with a thermostated cell holder and using a 1 mm path-length quartz cell. CD spectra were obtained from aliquots withdrawn from the aggregation mixtures at the times indicated, and spectra were measured at the indicated temperature (25°C or 55°C). The secondary structure content was estimated from each spectrum by using the CDPro software package (58).

Attenuated total reflection Fourier transform infrared spectroscopy

Attenuated total reflection Fourier transform infrared (ATR-FTIR) spectra were recorded using a Bruker Equinox55 spectrometer (Ettlingen, Germany) equipped with a liquid N_2-cooled mercury cadmium telluride detector and purged with a continuous flow of N_2 gas. A BioATRCell II accessory from Bruker was used as a sampling system. Spectra were measured at the indicated temperature (25°C or 55°C). For each sample, 256 interferograms were accumulated at a spectral resolution of 2 cm^{-1}. Buffer spectra were recorded under identical conditions to those of the protein samples and automatically subtracted from the spectra of the proteins using Bruker Protein Dynamics software. Spectra were baselined and then normalized such that the minimally occurring y-value was set to 0 and the maximally occurring y-value to 2 absorbance units.

Transmission electron microscopy

Samples were applied to Formvar-carbon-coated nickel grids (400 mesh), negatively stained with 2% (w/v) uranyl acetate, and viewed in a Philips CM100 transmission electron microscope (Eindhoven, The Netherlands) operating at 80 kV.

RESULTS

Aggregation of AcP after destabilization by heat

Solutions of AcP in 50 mM sodium acetate, pH 5.5, were heated at 55°C for 1 h. From the previously described

thermal denaturation behavior (59), it is possible to infer that under these conditions the native state is at least partially populated and is in equilibrium with the denatured state. Indeed, AcP maintains a significant degree of activity under these conditions. CD and ATR-FTIR spectra confirm the presence of a nonnative state populated to a significant extent (Figs. 1 *a* and 2 *a*). The completely unfolded state formed at higher temperatures was found to convert rapidly into amorphous aggregates that lack any secondary structure elements detectable by CD or ATR-FTIR and was therefore not studied further. TFE was added to the destabilized samples at 55°C to give final concentrations of TFE of 5%, 10%, 15%, and 25% (v/v) and 0.4 mg/ml of AcP.

CD spectra, each representing a weighted average of an ensemble of different conformational states, were recorded 1 min after the addition of the various concentrations of TFE to the samples at 55°C (Fig. 1 *a*). The extent of α-helical structure in the partially unfolded protein was found to increase as the concentration of TFE increases to 25% (Fig. 1 *a*, Table 1), in accord with previous observations on the effect of TFE on the structural properties of AcP at lower temperature (19). A control experiment performed at a concentration of protein substantially lower than 0.4 mg/ml (0.08 mg/ml) to reduce the aggregation rate sufficiently to allow measurements to be made in 5% TFE, demonstrates that after 1 min all the structural transitions induced in the monomeric protein at 55°C are complete.

The propensity for the protein samples to form aggregates under these conditions was assessed by using ThT, a dye that specifically binds to ordered β-sheet aggregates and, notably, to amyloid fibrils (60). In the absence of TFE, no increase in ThT fluorescence was observed even after 60 h of incubation at 55°C (Fig. 3 *a*). By contrast, exponential increases in ThT intensity were observed in the solutions to which TFE was added (Fig. 3 *a*). The rates are significantly slower in 15% and 25% TFE than in 5% and 10% TFE (Fig. 3 *a*) although the fluorescence intensities at the end of the exponential phases are comparable in all the samples.

The finding that the rate of aggregation decreases as the TFE concentration is increased from 5% to 25% (v/v) suggests that an increase in α-helical structure inhibits aggregation. CD spectra of the samples recorded after 1 day, however, all show a decrease in the α-helical content and a corresponding shift toward β-structure (shown by an increase in ellipticity at ~216 nm) characteristic of aggregate formation (Fig. 4, *a* and *b*). In addition, differences in the ellipticity of the samples at different TFE concentrations are due at least in part to a decrease in the intensity resulting from scattering by the aggregated species (13).

ATR-FTIR spectra were recorded after incubation of the solutions for 1 week under the conditions described above. Unlike the spectra of the samples incubated at 25°C or 55°C in the absence of TFE, the spectra of all the samples in 5–25% TFE, 55°C, exhibit an intense peak between 1630 and

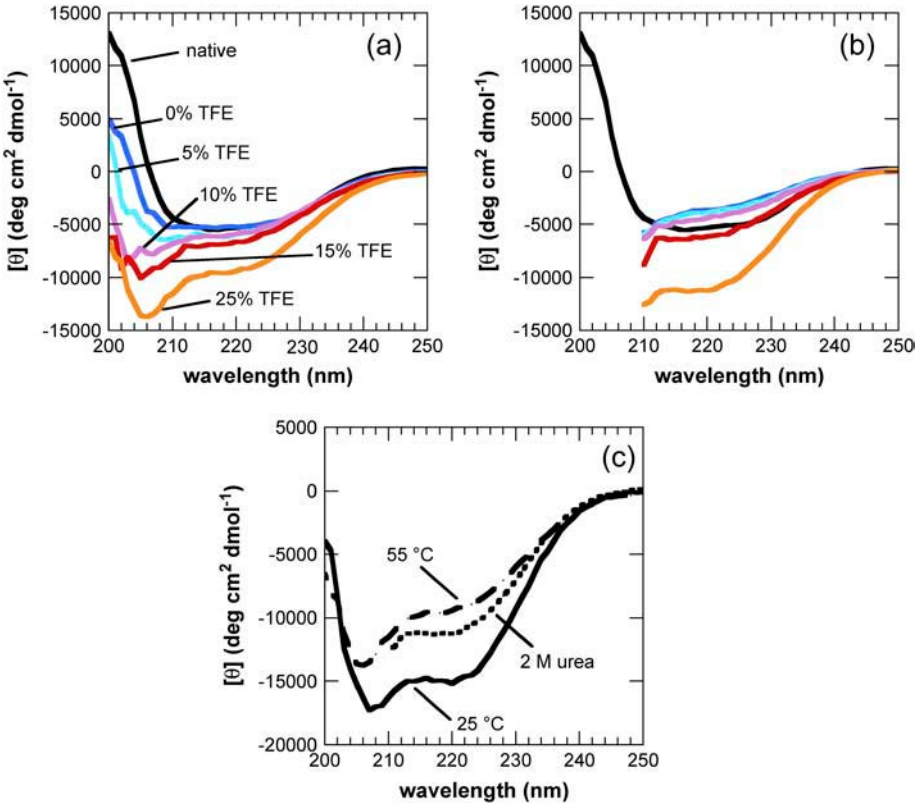

FIGURE 1 Far-UV CD spectra of different initial states from which AcP aggregates. Spectra were acquired 1 min after the addition of different concentrations of TFE to AcP samples preincubated at 55°C (*a*) and in 2 M urea at 25°C (*b*). In *b*, the F94L mutant was used instead of wild-type (wt) AcP (see text). Black indicates the native state at 25°C in the absence of TFE and urea; the colors indicate different TFE concentrations added to the destabilized state at 55°C or 2 M urea: blue, 0% TFE; cyan, 5% TFE; purple, 10% TFE; red, 15% TFE; orange, 25% TFE. (*c*) Comparison of the spectra of samples at 25°C (*solid line*), 55°C (*dashed line*), and in 2 M urea, 25°C (*dotted line*), all obtained in the presence of 25% TFE.

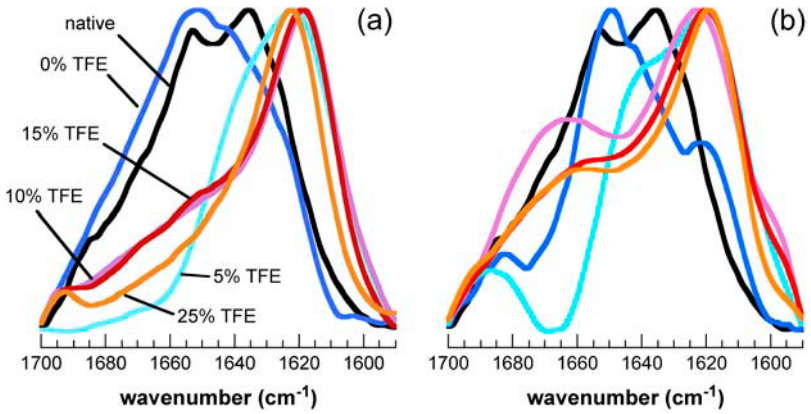

FIGURE 2 ATR-FTIR spectra of different aggregated states of AcP. Amide I′ spectra were acquired 1 week after the addition of different concentrations of TFE to samples preincubated at 55°C (*a*) and in 2 M urea at 25°C (*b*). In *b*, the F94L mutant was used instead of wt AcP. The color code is the same as in Fig. 1. Spectra were normalized to the minimum and maximum absorbance values in each experiment.

1615 cm^{-1} in the amide I′ region, implying, in agreement with the CD spectra, that the aggregated species possess extensive β-sheet structure (Fig. 2 *a*). Significantly, this type of infrared spectrum has been shown to be characteristic of amyloid fibrils (71). In addition, transmission electron microscopy (TEM) images taken after 1 week at 5%, 10%, and 15% TFE show the presence of well-defined fibrillar structures (Fig. 5, *a* and *b*) with diameters of ~10 nm (Fig. 5 *a*, *inset*), consistent with the data for the majority of well-defined amyloid fibrils formed by other proteins (62). At 25% TFE the aggregates appear to be less regularly structured.

Aggregation of AcP after destabilization by mutation and urea

The aggregates of AcP formed at a protein concentration of 0.4 mg/ml in 25% (v/v) TFE at pH 5.5 and 25°C were found to dissolve at urea concentrations higher than 2.5 M. As the midpoint of the urea denaturation of wild-type AcP under similar conditions of pH and temperature is ~4.5 M urea (59), we used a destabilized mutant, F94L, to enable AcP to be unfolded under conditions that still promote aggregation. The aggregation rate of this mutant from the partially unfolded state formed in 25% TFE has been found to be very similar to that of the wild-type protein (19), and CD analysis confirms that F94L AcP is unfolded in 2 M urea in the absence of TFE (Fig. 1 *b*, Table 1). Samples of F94L AcP were therefore incubated in 2 M urea, 50 mM sodium acetate, pH 5.5, 25°C for 1 h to ensure unfolding was complete. Different concentrations of TFE were then added to obtain solutions of 0.4 mg/ml of protein in 2 M urea containing 5%, 10%, 15%, and 25% (v/v) TFE. The CD spectrum acquired after 1 min after the addition of 5% TFE is very similar to that of the unfolded sample in the absence of TFE (Fig. 1 *b*), but there is a progressive increase in the extent of α-helical structure as TFE concentration is increased to 10%, 15%, and 25% (Fig. 1 *b*, Table 1).

The kinetics of aggregation under these conditions was again measured using ThT fluorescence (Fig. 3 *b*). In the absence of TFE, no aggregation was observed for more than 1 week, whereas in its presence aggregation is almost complete at all the concentrations examined here (Fig. 3 *b*).

TABLE 1 Comparison of secondary structure content* before aggregation and half time for the aggregation reaction†

	% α-helix	% β-sheet	% turn	% random	$t_{½}$ (min)
wt 0%TFE 25°C	20.3 ± 5.0	31.4 ± 5.0	19.9 ± 5.0	28.4 ± 5.0	
wt 25%TFE 25°C	43.0 ± 5.0	11.4 ± 5.0	15.9 ± 5.0	29.7 ± 5.0	9 ± 3§
wt 0%TFE 55°C	18.4 ± 5.0	30.0 ± 5.0	20.1 ± 5.0	31.5 ± 5.0	
wt 5%TFE 55°C	20.7 ± 5.0	26.9 ± 5.0	21.4 ± 5.0	31.0 ± 5.0	51 ± 5
wt 10%TFE 55°C	17.5 ± 5.0	26.8 ± 5.0	19.6 ± 5.0	36.1 ± 5.0	45 ± 5
wt 15%TFE 55°C	19.3 ± 5.0	22.5 ± 5.0	18.9 ± 5.0	39.3 ± 5.0	230 ± 10
wt 25%TFE 55°C	33.6 ± 5.0	14.3 ± 5.0	19.6 ± 5.0	32.5 ± 5.0	1430 ± 60
F94L 0%TFE 2 M urea‡ 25°C	6.9 ± 5.0	16.7 ± 5.0	11.2 ± 5.0	65.2 ± 5.0	
F94L 5%TFE 2 M urea‡ 25°C	7.1 ± 5.0	16.8 ± 5.0	11.3 ± 5.0	64.8 ± 5.0	3540 ± 120
F94L 10%TFE 2 M urea‡ 25°C	7.3 ± 5.0	18.6 ± 5.0	10.5 ± 5.0	63.6 ± 5.0	2520 ± 90
F94L 15%TFE 2 M urea‡ 25°C	17.5 ± 5.0	15.5 ± 5.0	13.1 ± 5.0	53.9 ± 5.0	1230 ± 60
F94L 25%TFE 2 M urea‡ 25°C	35.6 ± 5.0	13.3 ± 5.0	18.0 ± 5.0	33.1 ± 5.0	1920 ± 75

*Obtained using the CDPro software package (58). An error of ± 5.0 is estimated for each value.
†Expressed as half times of the maximum value of the fluorescence intensity obtained within the timescale shown in Fig. 3.
‡The effect on the spectra at wavelengths lower than 210 nm resulting from the presence of urea allows only a qualitative estimate of the secondary structure content to be made.
§Values extrapolated from Chiti et al. (57).

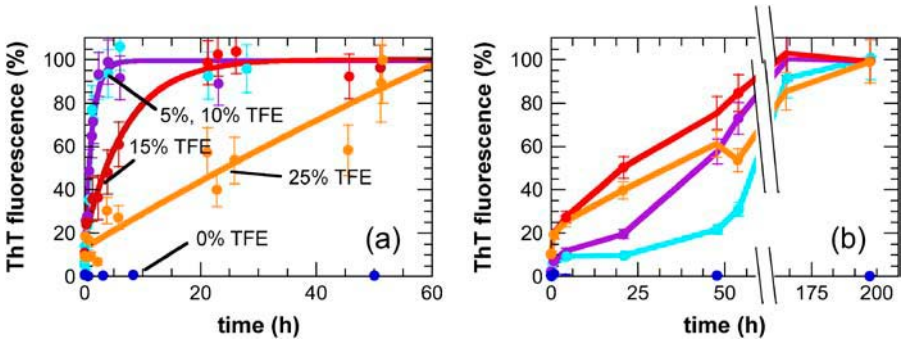

FIGURE 3 Aggregation kinetics of AcP from different partially unfolded states. Aggregation was monitored by ThT fluorescence after the addition of different concentrations of TFE to samples preincubated at 55°C (*a*) and in 2 M urea, 25°C (*b*). In *b*, the F94L mutant was used instead of wt AcP. The color code is the same as in Fig. 1. The data points were normalized to attribute 100% intensity to the maximum value of ThT fluorescence intensity observed at the end of each experiment. The solid lines in *a* represent the single exponential functions which provide the best fits to the data.

Compared to the aggregation process followed at 55°C in the absence of urea, the kinetics of aggregation in urea at 25°C are dramatically slower at equivalent concentrations of TFE (Fig. 3). In addition, aggregation in urea proceeds with nonexponential kinetics, and at 5% TFE a well-defined lag phase is clearly evident. This lag phase becomes shorter as the TFE concentration is increased (Fig. 3 *b*). Lag phases are commonly observed in aggregation reactions and indicate the need for a nucleation step before the rapid growth phase. The lack of a lag phase for AcP aggregation under most conditions indicates that the nucleation process is not rate determining. The fact that there is a lag phase for the aggregation of the F94L mutant in the presence of urea suggests that nucleation is now rate determining for this AcP variant, perhaps because the stability of the initial oligomers is decreased under these conditions.

After 1 week of incubation, a decrease in intensity was observed in the CD spectra of the sample incubated in 5% TFE, whereas a clear shift from a typically α-helical to a β-sheet spectrum was found for the samples incubated at higher TFE concentrations (Fig. 4, *c* and *d*). Analysis of these samples using ATR-FTIR shows spectra very similar to those observed for the samples incubated at 55°C, with an intense peak at ~1615 cm^{-1}, indicative of a high β-structure content in the protein aggregates (Fig. 2 *b*). However, in the presence of only 5% TFE, a strong peak at ~1650 cm^{-1} and the lack of intensity at 1665 cm^{-1}, attributable to turn structures, indicate that the protein is largely unstructured

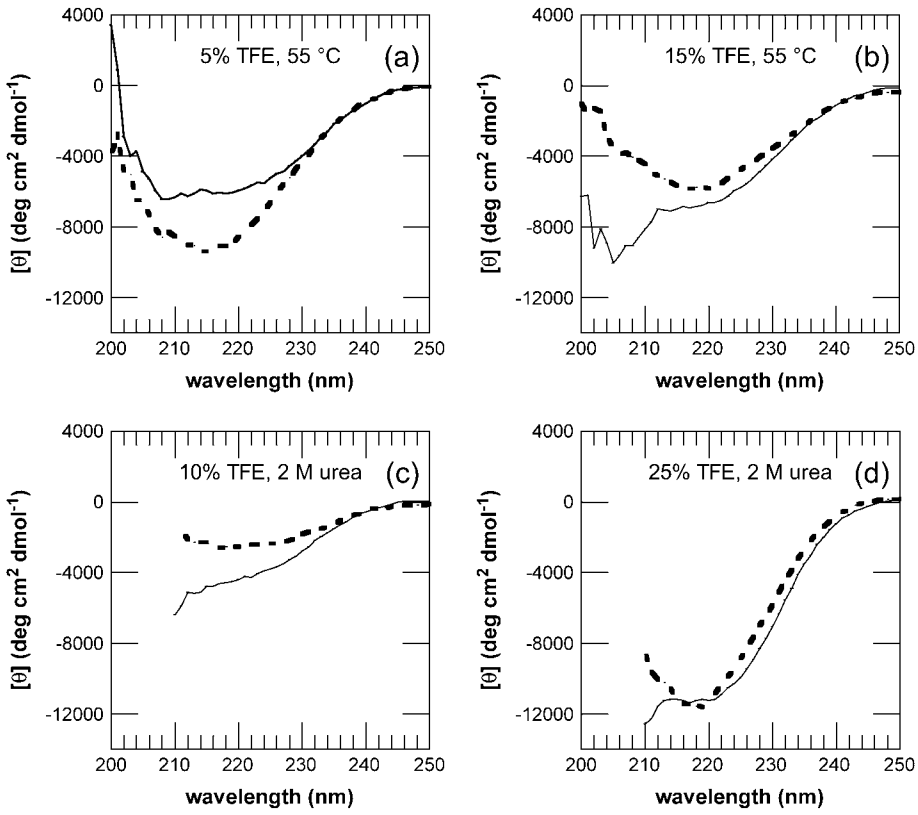

FIGURE 4 Far-UV CD spectra of AcP before and after aggregation. Spectra were acquired after 1 min (*solid line*), 1 day (*dotted line*, *a* and *b*), or 1 week (*dotted line*, *c* and *d*) after the addition of different concentrations of TFE to samples preincubated at 55°C (*a* and *b*) and in 2 M urea (*c* and *d*). In *c* and *d*, the F94L mutant was used instead of wt AcP. The samples were incubated in 5% (*a*), 10% (*c*), 15% (*b*), and 25% (*d*) TFE. A similar shift of the peak to wavelengths between 210 and 220 nm was observed also for the samples incubated in 15–25% TFE at 55°C, and 5–10% TFE in 2 M urea.

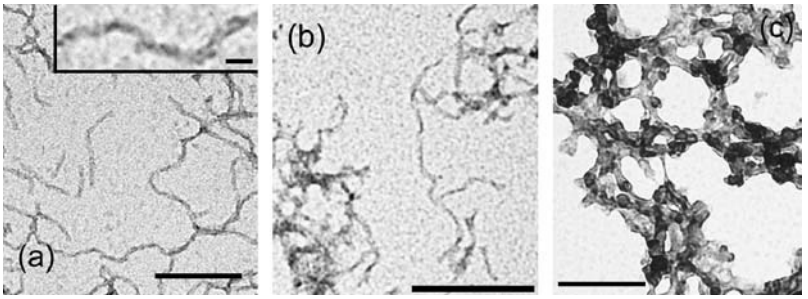

FIGURE 5 Aggregates of AcP observed by TEM. The protein was incubated in 5% (*a*) and 15% TFE (*b*) at 55°C or in 10% TFE and 2 M urea at 25°C (*c*), and images were acquired after 1 week. In *c*, the F94L mutant was used instead of wt AcP. An expanded image is shown in the inset (*a*). The scale bars at the bottom of *a* and *c* correspond to 100 nm; those in *b* and in the inset correspond to 50 nm and 10 nm, respectively.

under these conditions. Despite the relatively high content of β-structure and the ability to bind to ThT, the aggregates formed in higher concentrations of TFE (10–25%) do not have the typical morphology of amyloid fibrils, although a form of filamentous structure is suggested by TEM images of samples incubated for 1 week (Fig. 5 *c*).

Effects of heat and urea on the monomeric precursors to aggregate formation

Since elevated temperature and the presence of urea perturb intramolecular as well as intermolecular interactions, a detailed comparison of the aggregation process at the same TFE concentrations under these different conditions is unlikely to be meaningful. It is possible, however, to compare the CD spectra of partially unfolded AcP in 25% TFE under these different conditions. Comparison of the species present in 25% TFE at 25°C and 55°C shows that the extent of α-helical structure is significantly greater in the samples at 25°C than at 55°C, indicating that hydrogen bonding is less dominant at higher temperatures (Fig. 1 *c*, Table 1). The CD spectrum of the F94L mutant of AcP after 1min in 25% TFE, 25°C, 2 M urea, shows an α-helical content lower than that of wild-type AcP under the same conditions in the absence of urea but slightly higher than that found at 55°C in the absence of urea (Fig. 1 *c*, Table 1). Under the former conditions, however, aggregation is dramatically slower, indicating the absence of a straightforward correlation between aggregation rate and α-helical content within the initial conformational state. This result indicates also that urea is likely to destabilize the formation of hydrogen bonds.

Both heat and urea are also likely to affect the strength of the hydrophobic effect on intermolecular interactions. A rough comparison of the half times ($t_{1/2}$) of the maximum values of fluorescence intensity obtained within the timescale used here with respect to the concentration of TFE results in the order $0 \gg 5 \sim 10 < 15 < 25\%$ TFE for experiments carried out at 55°C and $0 \gg 5 > 10 > 15 < 25\%$ TFE for experiments carried out in 2 M urea, 25°C (Table 1). The fact that the minimum $t_{1/2}$ of aggregation is 5% TFE at 55°C but is 15% TFE in 2 M urea, 25°C, and the finding that changes in hydrophobicity through mutations can influence the aggregation rate of a polypeptide (57), suggest that this shift could be due to a larger decrease in the hydrophobic effect in urea rather than to the changes in temperature.

DISCUSSION

Solution conditions are critical for aggregation

Partial or complete unfolding of the native state of AcP is not by itself sufficient to promote aggregation during the relatively short timescale used here (1 week). Under conditions where the protein is partially (55°C) or effectively completely unfolded (2 M urea) the protein does not aggregate at a significant rate in the absence of TFE. This result can be rationalized by considering that denaturant conditions that are strong enough to unfold the protein substantially, such as high temperature or addition of urea, not only destabilize intramolecular interactions but also the analogous intermolecular interactions. Thus, weaker hydrophobic interactions are likely to result both in reduced compactness and increased solubility.

Under such conditions, the addition of TFE (a solvent less polar than water and a weaker hydrogen bond competitor) appears to promote the formation of ordered aggregates by strengthening the interactions that stabilize intermolecular β-sheet structure as well as intramolecular β-turns and helical structure (43,48,53,63). We can therefore conclude that under the conditions used here, the formation of intermolecular hydrogen bonds is likely to be an important driving force for the aggregation of denatured AcP. The effect of TFE at concentrations ranging from 5% to 25% is therefore to change the balance of factors that favor aggregation relative to solubility and to provide an environment which favors strong intermolecular interactions.

If the extent of α-helical structure present in the partially unfolded state reflects the degree to which intramolecular peptide hydrogen bonds are stabilized under different conditions, then high temperatures and addition of urea both weaken the strength of hydrogen bonds as shown in Fig. 1 *c*. To aggregate, a protein such as AcP requires at least partial unfolding to expose the polypeptide main chain and hydrophobic residues to enable strong intermolecular interactions to develop; the compact native states of globular proteins have been selected by evolution to avoid aggregation primarily by the burial of their hydrophobic groups and the

judicious placement of charged and polar residues on the surface (1). Importantly, the observation that aggregation often occurs from a partially, rather than fully, unfolded state does not indicate that the presence of residual structure is important to promote amyloid aggregation. Rather, the structure present in the partially unfolded state may simply be a consequence of the fact that the solution conditions promoting aggregation are also those that will stabilize intramolecular (often native-like) structure as the types of interactions involved in the two processes are essentially identical. This observation suggests, therefore, that the nature of the structure of the initial conformational state may be of much less importance than factors such as hydrophobicity, net charge, and β-sheet propensity (35).

Very different initial states can result in very similar aggregated states

In this study, we were able to generate aggregation-prone partially unfolded states of AcP with very different secondary structure contents by variation of the solution conditions. The essential nature of the resulting amyloid-like aggregates (fibrillar morphology, extensive β-structure, and ThT binding) is preserved although the exact details of the intermolecular interactions undoubtedly differ with the conditions. Examination of the literature provides further evidence for this conclusion. For example, the protein lysozyme has been shown to be able to form amyloid fibrils that appear to be closely similar under many different conditions, including the presence of denaturants such as guanidine hydrochloride (64) and ethanol (65), application of hydrostatic pressure (23), reduction of disulfide bonds (66), partial proteolytic degradation (67), low pH values, and high temperatures (21). As in this study, however, the partially unfolded states from which aggregation is initiated have rather distinct structural characteristics that are becoming increasingly evident from the ability to carry out detailed studies of nonnative states of proteins (68,69).

The formation of both fibrillar and nonfibrillar aggregates, each of which can have a high content of β-sheet structure, appears from the results of this study to be substantially independent of the overall initial secondary structure content. As shown schematically for AcP in Fig. 6, the initial monomeric species can posses a mixture of α-helical and β-sheet character (5% TFE, 55°C) or be rich in α-helical (25% TFE, 55°C) or highly disordered (F94L mutant, 10% TFE, 2 M urea) structure. These results also demonstrate that the presence of a particular type of secondary structure is not mandatory for the aggregation process of AcP to give rise to amyloid fibrils. An increase of TFE concentration from 5–10% to 15–25% at 55°C results in an increase in α-helical structure and a slower aggregation process; the latter can be attributable to the fact that α-helices involve intramolecular hydrogen bonds and therefore their presence reduces the probability of forming intermolecular interactions. In support of this conclusion, it has been shown that mutations in proteins that stabilize α-helical structure can slow down the process of aggregation from their denatured states (70,71).

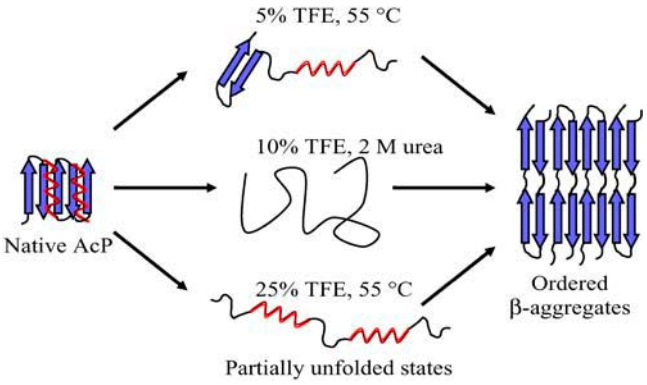

FIGURE 6 Schematic representation of the aggregation process of AcP from different partially unfolded states. The globular native state of AcP is converted into a partially unfolded state that can contain a mixture of α-helical and β-sheet structure (5% TFE, 55°C), a high content of α-helical (25% TFE, 55°C) or disordered (F94L, 10% TFE, 2 M urea, 25°C) structure. Despite the differences in the conditions, all of these partially unfolded states can be converted into ordered fibrillar aggregates containing a highly organized β-sheet structure.

Despite such considerations, the regions of a polypeptide sequence involved in triggering the aggregation process from very different initial states could well differ significantly. These regions are in general likely to be those that are relatively flexible and not involved in strong intramolecular interactions (18,22,72–74). Interestingly, the regions of the sequence of AcP in 25% TFE found to be exposed to solvent from limited proteolysis studies match those previously identified to be critical in the rate-determining steps of aggregation from protein engineering approaches (39,57). Nevertheless, different conditions may cause different regions to have such characteristics and therefore to be those that initiate the aggregation process. In addition, it has been shown that specific features of the amino acid sequence, as well as the solution conditions, can significantly influence the aggregation rate (35,75,76). Such considerations can explain, at least in part, why partially unfolded states of AcP formed under very different conditions have very different aggregation rates. In accord with previous studies, the different precursor states that result from different solution conditions can generate fibrillar or nonfibrillar aggregates with similar β-sheet content but with distinct morphological features, for example flat ribbons as compared to more cylindrical forms of amyloid fibrils (34,77). One contribution to such effects could be that different parts of the protein are involved in the dominant intermolecular interactions under the different conditions. Thus, even when interactions involving the polypeptide backbone are the major determinants of amyloid structure through the formation of intermolecular hydrogen bonds, the side chains can still exert a significant influence on the features of the resulting assembly

(10,34,35). Although much remains to be learned about the way that side-chain interactions and solution conditions influence the morphology of the aggregates, a more profound understanding of the basic principles that underlie the process of protein aggregation will undoubtedly shed further light both on this issue and on related phenomena, such as the way in which the details of protein aggregation can contribute to human disease and its treatment.

We thank Reto Bader, Massimo Stefani, and Niccolò Taddei for valuable discussions.

This work was supported by grants from the Wellcome Trust, from the European Commission (Research Directorates, project ''Protein (mis)folding'' proposal No. RTN2-2001-00364), and from the Italian MIUR (PRIN 2003025755_003).

REFERENCES

1. Dobson, C. M. 2003. Protein folding and misfolding. *Nature*. 426: 884–890.
2. Walsh, D. M., and D. J. Selkoe. 2004. Oligomers on the brain: the emerging role of soluble protein aggregates in neurodegeneration. *Protein Pept. Lett.* 11:213–228.
3. Buxbaum, J. N. 2004. The systemic amyloidoses. *Curr. Opin. Rheumatol.* 16:67–75.
4. Pepys, M. B. 2001. Pathogenesis, diagnosis and treatment of systemic amyloidosis. *Philos. Trans. R. Soc. Lond. B Biol. Sci.* 356:203–210 (discussion 210–201).
5. Stefani, M., and C. M. Dobson. 2003. Protein aggregation and aggregate toxicity: new insights into protein folding, misfolding diseases and biological evolution. *J. Mol. Med.* 81:678–699.
6. Caughey, B., and P. T. Lansbury Jr. 2003. Protofibrils, pores, fibrils, and neurodegeneration: separating the responsible protein aggregates from the innocent bystanders. *Annu. Rev. Neurosci.* 26:267–298.
7. Bucciantini, M., E. Giannoni, F. Chiti, F. Baroni, L. Formigli, J. Zurdo, N. Taddei, G. Ramponi, C. M. Dobson, and M. Stefani. 2002. Inherent toxicity of aggregates implies a common mechanism for protein misfolding diseases. *Nature*. 416:507–511.
8. Kayed, R., E. Head, J. L. Thompson, T. M. McIntire, S. C. Milton, C. W. Cotman, and C. G. Glabe. 2003. Common structure of soluble amyloid oligomers implies common mechanism of pathogenesis. *Science*. 300:486–489.
9. Sunde, M., and C. Blake. 1997. The structure of amyloid fibrils by electron microscopy and x-ray diffraction. *Adv. Protein Chem.* 50:123–159.
10. Chamberlain, A. K., C. E. MacPhee, J. Zurdo, L. A. Morozova-Roche, H. A. Hill, C. M. Dobson, and J. J. Davis. 2000. Ultrastructural organization of amyloid fibrils by atomic force microscopy. *Biophys. J.* 79: 3282–3293.
11. Makin, O. S., and L. C. Serpell. 2002. Examining the structure of the mature amyloid fibril. *Biochem. Soc. Trans.* 30:521–525.
12. Guijarro, J. I., M. Sunde, J. A. Jones, I. D. Campbell, and C. M. Dobson. 1998. Amyloid fibril formation by an SH3 domain. *Proc. Natl. Acad. Sci. USA*. 95:4224–4228.
13. Chiti, F., P. Webster, N. Taddei, A. Clark, M. Stefani, G. Ramponi, and C. M. Dobson. 1999. Designing conditions for in vitro formation of amyloid protofilaments and fibrils. *Proc. Natl. Acad. Sci. USA*. 96: 3590–3594.
14. Fandrich, M., and C. M. Dobson. 2002. The behaviour of polyamino acids reveals an inverse side chain effect in amyloid structure formation. *EMBO J.* 21:5682–5690.
15. Uversky, V. N., and A. L. Fink. 2004. Conformational constraints for amyloid fibrillation: the importance of being unfolded. *Biochim. Biophys. Acta.* 1698:131–153.
16. Hurle, M. R., L. R. Helms, L. Li, W. Chan, and R. Wetzel. 1994. A role for destabilizing amino acid replacements in light-chain amyloidosis. *Proc. Natl. Acad. Sci. USA*. 91:5446–5450.
17. McCutchen, S. L., Z. Lai, G. J. Miroy, J. W. Kelly, and W. Colon. 1995. Comparison of lethal and nonlethal transthyretin variants and their relationship to amyloid disease. *Biochemistry.* 34:13527–13536.
18. Booth, D. R., M. Sunde, V. Bellotti, C. V. Robinson, W. L. Hutchinson, P. E. Fraser, P. N. Hawkins, C. M. Dobson, S. E. Radford, C. C. Blake, and M. B. Pepys. 1997. Instability, unfolding and aggregation of human lysozyme variants underlying amyloid fibrillogenesis. *Nature*. 385:787–793.
19. Chiti, F., N. Taddei, M. Bucciantini, P. White, G. Ramponi, and C. M. Dobson. 2000. Mutational analysis of the propensity for amyloid formation by a globular protein. *EMBO J.* 19:1441–1449.
20. Niraula, T. N., K. Haraoka, Y. Ando, H. Li, H. Yamada, and K. Akasaka. 2002. Decreased thermodynamic stability as a crucial factor for familial amyloidotic polyneuropathy. *J. Mol. Biol.* 320:333–342.
21. Krebs, M. R., D. K. Wilkins, E. W. Chung, M. C. Pitkeathly, A. K. Chamberlain, J. Zurdo, C. V. Robinson, and C. M. Dobson. 2000. Formation and seeding of amyloid fibrils from wild-type hen lysozyme and a peptide fragment from the beta-domain. *J. Mol. Biol.* 300:541–549.
22. Moraitakis, G., and J. M. Goodfellow. 2003. Simulations of human lysozyme: probing the conformations triggering amyloidosis. *Biophys. J.* 84:2149–2158.
23. De Felice, F. G., M. N. Vieira, M. N. Meirelles, L. A. Morozova-Roche, C. M. Dobson, and S. T. Ferreira. 2004. Formation of amyloid aggregates from human lysozyme and its disease-associated variants using hydrostatic pressure. *FASEB J.* 18:1099–1101.
24. Ferrao-Gonzales, A. D., S. O. Souto, J. L. Silva, and D. Foguel. 2000. The preaggregated state of an amyloidogenic protein: hydrostatic pressure converts native transthyretin into the amyloidogenic state. *Proc. Natl. Acad. Sci. USA*. 97:6445–6450.
25. Khurana, R., J. R. Gillespie, A. Talapatra, L. J. Minert, C. Ionescu-Zanetti, I. Millett, and A. L. Fink. 2001. Partially folded intermediates as critical precursors of light chain amyloid fibrils and amorphous aggregates. *Biochemistry*. 40:3525–3535.
26. Zurdo, J., J. I. Guijarro, J. L. Jimenez, H. R. Saibil, and C. M. Dobson. 2001. Dependence on solution conditions of aggregation and amyloid formation by an SH3 domain. *J. Mol. Biol.* 311:325–340.
27. Bousset, L., N. H. Thomson, S. E. Radford, and R. Melki. 2002. The yeast prion Ure2p retains its native alpha-helical conformation upon assembly into protein fibrils in vitro. *EMBO J.* 21:2903–2911.
28. Lee, A. S., C. Galea, E. L. DiGiammarino, B. Jun, G. Murti, R. C. Ribeiro, G. Zambetti, C. P. Schultz, and R. W. Kriwacki. 2003. Reversible amyloid formation by the p53 tetramerization domain and a cancer-associated mutant. *J. Mol. Biol.* 327:699–709.
29. Plakoutsi, G., N. Taddei, M. Stefani, and F. Chiti. 2004. Aggregation of the acylphosphatase from sulfolobus solfataricus: the folded and partially unfolded states can both be precursors for amyloid formation. *J. Biol. Chem.* 279:14111–14119.
30. Eakin, C. M., F. J. Attenello, C. J. Morgan, and A. D. Miranker. 2004. Oligomeric assembly of native-like precursors precedes amyloid formation by beta-2 microglobulin. *Biochemistry*. 43:7808–7815.
31. Lai, Z., W. Colon, and J. W. Kelly. 1996. The acid-mediated denaturation pathway of transthyretin yields a conformational intermediate that can self-assemble into amyloid. *Biochemistry*. 35:6470–6482.
32. Canet, D., A. M. Last, P. Tito, M. Sunde, A. Spencer, D. B. Archer, C. Redfield, C. V. Robinson, and C. M. Dobson. 2002. Local cooperativity in the unfolding of an amyloidogenic variant of human lysozyme. *Nat. Struct. Biol.* 9:308–315.
33. McParland, V. J., A. P. Kalverda, S. W. Homans, and S. E. Radford. 2002. Structural properties of an amyloid precursor of beta(2)-microglobulin. *Nat. Struct. Biol.* 9:326–331.
34. Smith, D. P., S. Jones, L. C. Serpell, M. Sunde, and S. E. Radford. 2003. A systematic investigation into the effect of protein destabilisation on beta 2-microglobulin amyloid formation. *J. Mol. Biol.* 330:943–954.

35. Chiti, F., M. Stefani, N. Taddei, G. Ramponi, and C. M. Dobson. 2003. Rationalization of the effects of mutations on peptide and protein aggregation rates. *Nature*. 424:805–808.

36. Calamai, M., N. Taddei, M. Stefani, G. Ramponi, and F. Chiti. 2003. Relative influence of hydrophobicity and net charge in the aggregation of two homologous proteins. *Biochemistry*. 42:15078–15083.

37. Ahmad, A., I. S. Millett, S. Doniach, V. N. Uversky, and A. L. Fink. 2003. Partially folded intermediates in insulin fibrillation. *Biochemistry*. 42:11404–11416.

38. Hoyer, W., D. Cherny, V. Subramaniam, and T. M. Jovin. 2004. Impact of the acidic C-terminal region comprising amino acids 109–140 on alpha-synuclein aggregation in vitro. *Biochemistry*. 43:16233–16242.

39. Monti, M., B. L. Garolla di Bard, G. Calloni, F. Chiti, A. Amoresano, G. Ramponi, and P. Pucci. 2004. The regions of the sequence most exposed to the solvent within the amyloidogenic state of a protein initiate the aggregation process. *J. Mol. Biol.* 336:253–262.

40. Kayed, R., J. Bernhagen, N. Greenfield, K. Sweimeh, H. Brunner, W. Voelter, and A. Kapurniotu. 1999. Conformational transitions of islet amyloid polypeptide (IAPP) in amyloid formation in vitro. *J. Mol. Biol.* 287:781–796.

41. Bouchard, M., J. Zurdo, E. J. Nettleton, C. M. Dobson, and C. V. Robinson. 2000. Formation of insulin amyloid fibrils followed by FTIR simultaneously with CD and electron microscopy. *Protein Sci.* 9:1960–1967.

42. Kirkitadze, M. D., M. M. Condron, and D. B. Teplow. 2001. Identification and characterization of key kinetic intermediates in amyloid beta-protein fibrillogenesis. *J. Mol. Biol.* 312:1103–1119.

43. Fezoui, Y., and D. B. Teplow. 2002. Kinetic studies of amyloid beta-protein fibril assembly. Differential effects of alpha-helix stabilization. *J. Biol. Chem.* 277:36948–36954.

44. Andreola, A., V. Bellotti, S. Giorgetti, P. Mangione, L. Obici, M. Stoppini, J. Torres, E. Monzani, G. Merlini, and M. Sunde. 2003. Conformational switching and fibrillogenesis in the amyloidogenic fragment of apolipoprotein A-I. *J. Biol. Chem.* 278:2444–2451.

45. Klimov, D. K., and D. Thirumalai. 2003. Dissecting the assembly of Abeta16–22 amyloid peptides into antiparallel beta sheets. *Structure (Camb).* 11:295–307.

46. Srisailam, S., T. K. Kumar, D. Rajalingam, K. M. Kathir, H. S. Sheu, F. J. Jan, P. C. Chao, and C. Yu. 2003. Amyloid-like fibril formation in an all beta-barrel protein. Partially structured intermediate state(s) is a precursor for fibril formation. *J. Biol. Chem.* 278:17701–17709.

47. Gosal, W. S., A. H. Clark, and S. B. Ross-Murphy. 2004. Fibrillar beta-lactoglobulin gels: Part 1. Fibril formation and structure. *Biomacromolecules*. 5:2408–2419.

48. Munishkina, L. A., C. Phelan, V. N. Uversky, and A. L. Fink. 2003. Conformational behavior and aggregation of alpha-synuclein in organic solvents: modeling the effects of membranes. *Biochemistry*. 42:2720–2730.

49. Pallares, I., J. Vendrell, F. X. Aviles, and S. Ventura. 2004. Amyloid fibril formation by a partially structured intermediate state of alpha-chymotrypsin. *J. Mol. Biol.* 342:321–331.

50. Marcon, G., G. Plakoutsi, C. Canale, A. Relini, N. Taddei, C. M. Dobson, G. Ramponi, and F. Chiti. 2005. Amyloid formation from HypF-N under conditions in which the protein is initially in its native state. *J. Mol. Biol.* 347:323–335.

51. Buck, M. 1998. Trifluoroethanol and colleagues: cosolvents come of age. Recent studies with peptides and proteins. *Q. Rev. Biophys.* 31: 297–355.

52. Hirota-Nakaoka, N., and Y. Goto. 1999. Alcohol-induced denaturation of beta-lactoglobulin: a close correlation to the alcohol-induced alpha-helix formation of melittin. *Bioorg. Med. Chem.* 7:67–73.

53. Roccatano, D., G. Colombo, M. Fioroni, and A. E. Mark. 2002. Mechanism by which 2,2,2-trifluoroethanol/water mixtures stabilize secondary-structure formation in peptides: a molecular dynamics study. *Proc. Natl. Acad. Sci. USA*. 99:12179–12184.

54. Kumar, S., K. Modig, and B. Halle. 2003. Trifluoroethanol-induced beta → alpha transition in beta-lactoglobulin: hydration and cosolvent binding studied by 2H, 17O, and 19F magnetic relaxation dispersion. *Biochemistry.* 42:13708–13716.

55. Taddei, N., M. Stefani, F. Magherini, F. Chiti, A. Modesti, G. Raugei, and G. Ramponi. 1996. Looking for residues involved in the muscle acylphosphatase catalytic mechanism and structural stabilization: role of Asn41, Thr42, and Thr46. *Biochemistry.* 35:7077–7083.

56. van Nuland, N. A., F. Chiti, N. Taddei, G. Raugei, G. Ramponi, and C. M. Dobson. 1998. Slow folding of muscle acylphosphatase in the absence of intermediates. *J. Mol. Biol.* 283:883–891.

57. Chiti, F., N. Taddei, F. Baroni, C. Capanni, M. Stefani, G. Ramponi, and C. M. Dobson. 2002. Kinetic partitioning of protein folding and aggregation. *Nat. Struct. Biol.* 9:137–143.

58. Sreerama, N., and R. W. Woody. 2000. Estimation of protein secondary structure from circular dichroism spectra: comparison of CONTIN, SELCON, and CDSSTR methods with an expanded reference set. *Anal. Biochem.* 287:252–260.

59. Chiti, F., N. A. van Nuland, N. Taddei, F. Magherini, M. Stefani, G. Ramponi, and C. M. Dobson. 1998. Conformational stability of muscle acylphosphatase: the role of temperature, denaturant concentration, and pH. *Biochemistry*. 37:1447–1455.

60. LeVine 3rd, H. 1993. Thioflavine T interaction with synthetic Alzheimer's disease beta-amyloid peptides: detection of amyloid aggregation in solution. *Protein Sci.* 2:404–410.

61. Zandomeneghi, G., M. R. Krebs, M. G. McCammon, and M. Fandrich. 2004. FTIR reveals structural differences between native beta-sheet proteins and amyloid fibrils. *Protein Sci.* 13:3314–3321.

62. Serpell, L. C., M. Sunde, and C. C. Blake. 1997. The molecular basis of amyloidosis. *Cell. Mol. Life Sci.* 53:871–887.

63. Luo, Y., and R. L. Baldwin. 1998. Trifluoroethanol stabilizes the pH 4 folding intermediate of sperm whale apomyoglobin. *J. Mol. Biol.* 279: 49–57.

64. Vernaglia, B. A., J. Huang, and E. D. Clark. 2004. Guanidine hydrochloride can induce amyloid fibril formation from hen egg-white lysozyme. *Biomacromolecules*. 5:1362–1370.

65. Goda, S., K. Takano, Y. Yamagata, R. Nagata, H. Akutsu, S. Maki, K. Namba, and K. Yutani. 2000. Amyloid protofilament formation of hen egg lysozyme in highly concentrated ethanol solution. *Protein Sci.* 9: 369–375.

66. Cao, A., D. Hu, and L. Lai. 2004. Formation of amyloid fibrils from fully reduced hen egg white lysozyme. *Protein Sci.* 13:319–324.

67. Frare, E., P. Polverino De Laureto, J. Zurdo, C. M. Dobson, and A. Fontana. 2004. A highly amyloidogenic region of hen lysozyme. *J. Mol. Biol.* 340:1153–1165.

68. Klein-Seetharaman, J., M. Oikawa, S. B. Grimshaw, J. Wirmer, E. Duchardt, T. Ueda, T. Imoto, L. J. Smith, C. M. Dobson, and H. Schwalbe. 2002. Long-range interactions within a nonnative protein. *Science*. 295:1719–1722.

69. Kristjansdottir, S., K. Lindorff-Larsen, W. Fieber, C. M. Dobson, M. Vendruscolo, and F. M. Poulsen. 2005. Formation of native and nonnative interactions in ensembles of denatured ACBP molecules from paramagnetic relaxation enhancement studies. *J. Mol. Biol.* 347: 1053–1062.

70. Villegas, V., J. Zurdo, V. V. Filimonov, F. X. Aviles, C. M. Dobson, and L. Serrano. 2000. Protein engineering as a strategy to avoid formation of amyloid fibrils. *Protein Sci.* 9:1700–1708.

71. Taddei, N., C. Capanni, F. Chiti, M. Stefani, C. M. Dobson, and G. Ramponi. 2001. Folding and aggregation are selectively influenced by the conformational preferences of the alpha-helices of muscle acylphosphatase. *J. Biol. Chem.* 276:37149–37154.

72. Schormann, N., J. R. Murrell, and M. D. Benson. 1998. Tertiary structures of amyloidogenic and nonamyloidogenic transthyretin variants: new model for amyloid fibril formation. *Amyloid*. 5:175–187.

73. Fandrich, M., V. Forge, K. Buder, M. Kittler, C. M. Dobson, and S. Diekmann. 2003. Myoglobin forms amyloid fibrils by association of

unfolded polypeptide segments. *Proc. Natl. Acad. Sci. USA.* 100: 15463–15468.

74. Krishnan, R., and S. L. Lindquist. 2005. Structural insights into a yeast prion illuminate nucleation and strain diversity. *Nature.* 435:765–772.
75. DuBay, K. F., A. P. Pawar, F. Chiti, J. Zurdo, C. M. Dobson, and M. Vendruscolo. 2004. Prediction of the absolute aggregation rates of amyloidogenic polypeptide chains. *J. Mol. Biol.* 341:1317–1326.
76. Pawar, A. P., K. F. Dubay, J. Zurdo, F. Chiti, C. M. Dobson, and M. Vendruscolo. 2005. Prediction of ''aggregation-prone'' and ''aggregation-susceptible'' regions in proteins associated with neurodegenerative diseases. *J. Mol. Biol.* In press.
77. Petkova, A. T., R. D. Leapman, Z. Guo, W. M. Yau, M. P. Mattson, and R. Tycko. 2005. Self-propagating, molecular-level polymorphism in Alzheimer's beta-amyloid fibrils. *Science.* 307:262–265.